Chemical Mechanical Polishing of β-Ga_2O_3

Michael E. Liao,[1,*] Lezli Matto,[1] Dorian P. Luccioni,[1] Kenny Huynh,[1] Mark S. Goorsky[1,**]

[1]University of California Los Angeles, Los Angeles, California, 90095, United States
[*]meliao@ucla.edu, (310)825-8913
[**]goorsky@seas.ucla.edu, (310)206-0267

Keywords: Chemical Mechanical Polishing, Wide Bandgap Semiconductors, Gallium Oxide, X-ray Scattering

ABSTRACT

The chemical mechanical polishing of (010) β-Ga_2O_3 substrates was examined with emphasis on using x-ray scattering techniques with focus on the importance of sample mounting as well as diffraction conditions. Large instrumental broadening and/or poor sample mounting can obscure polish-induced damage when measuring X-ray rocking curves. Improperly mounting samples using excessive amounts of an adhesive (e.g. wax) introduces peak broadening in rocking curves by bending the substrates and inducing lattice strain and curvature. Furthermore, triple-axis diffraction measurements are more appropriate for measuring diffuse scatter intensity from subsurface damage than double-axis diffraction measurements due to intrinsic peak widths related measurement capabilities.

INTRODUCTION

β-Ga_2O_3 has been recognized as an appealing material for high power electronic applications due to its wide bandgap and high critical electric field [1,2]. Achieving smooth, sub-nm roughness surfaces is critical for realizing materials integration processes with β-Ga_2O_3, such as epitaxy and direct wafer bonding. However, the current literature is deficient in detailed studies on the chemical mechanical polishing (CMP) of β-Ga_2O_3, and key polishing parameters are often not described. Of the few detailed studies that currently exist, while smooth, sub-nm roughness was achieved [3,4], subsurface lattice damage was not assessed. Our previous work addressing the polishing of various III-V materials demonstrated that triple-axis X-ray diffraction (TAXRD) rocking curves are effective in analyzing subsurface lattice damage and optimizing various polishing parameters to completely remove the damage [5,6]. Subsurface damage manifests itself as diffuse scatter intensity, which is measured as FWXM (e.g. X = 0.1, 0.01, etc.), i.e. much below the full width at half maximum. However, samples must be carefully mounted on the diffractometer stage using a minimal amount of adhesive in order to accurately assess the presence of subsurface lattice damage. Improper mounting technique can lead to strain and curvature, which can introduce peak broadening which obscures polish-induced subsurface lattice damage. Furthermore, employing triple-axis is superior over double-axis when analyzing subsurface damage because of the smaller detector aperture. Using a broad detector aperture for measuring rocking curves (double-axis diffraction) convolutes broadening contributions along both the ω scanning axis and the ω:2θ scanning axis (which includes contributions from vertical coherence length, strain, and crystal truncation rod). Rocking curves measured using triple-axis diffraction deconvolutes the analysis because the narrow aperture does not capture contributions from the ω:2θ scanning axis.

EXPERIMENT

The rough surfaces of single-side polished 1.5 × 1.0 cm^2 (010) β-Ga_2O_3 substrates from Novel Crystal Technology, Inc. [7] were subject to CMP using a Logitech PM5 polisher. A poromeric polishing pad was used, 30 RPM pad rotation, and the applied pressure was less than 3 kPa – lower than what was employed in our previous work for polishing various III-V materials [5,6]. An alkaline 70-nm colloidal silica slurry was used. The rough surfaces of the substrates were polished to match the same pristine quality as the as-received polished side provided commercially.

A high-resolution Bruker-JV D1 diffractometer was used to measure rocking curves of the (020) β-Ga_2O_3 symmetric reflection. The X-ray source is Cu $K\alpha_1$ using a Göbel mirror [8] and a (110) channel-cut silicon crystal. Triple-axis measurements were performed using another (110) channel-cut silicon crystal as the analyzer crystal to reduce the detector aperture to ~10” [9-11], compared to double-axis measurements where the detector aperture is ~1400”. The incident X-ray beam width used was ~0.14 mm to reduce the contribution of lattice curvature on the rocking curves.

An FEI TITAN S/TEM was used to obtain high-angle annular dark field cross-sectional images, using an accelerating voltage of 300 keV. The samples were aligned along the [100] zone axis.

RESULTS AND DISCUSSION

The rough surfaces of the commercially available (010) β-Ga_2O_3 substrates were polished. These surfaces were rough due to wafer slicing, which not only damages the substrate surface but also introduce subsurface damage. As shown in the cross-sectional high-angle annular dark field image, both cracks and voids (dark contrast beneath the substrate surface) are observed. Zigzag contrast lines are also observed beneath the surface, which correspond to strained regions induced by the wafer slicing process. The damage from wafer slicing

induces lattice tilt, which can be directly measured with X-ray diffraction rocking curves. Figure 2 shows the symmetric (020) β-Ga_2O_3 triple-axis rocking curves for the unpolished wafer-sliced side compared to after polishing. Prior to polishing, the main substrate peak (at ω:2θ = 0") is broad with a FWHM of ~150" and an even broader peak is observed at -7600" away from the main substrate peak. The broad peak at -7600" corresponds to a low-angle grain boundary, which indicates that the wafer slicing process heavily distorts the lattice beneath the substrate surface. After removing the damaged material by CMP, both smooth surfaces (~0.3 nm rms roughness) and damage-free substrates were obtained. As shown in Figure 2, narrow rocking curves were obtained with a FWHM of 13" and FW(0.001)M of 130".

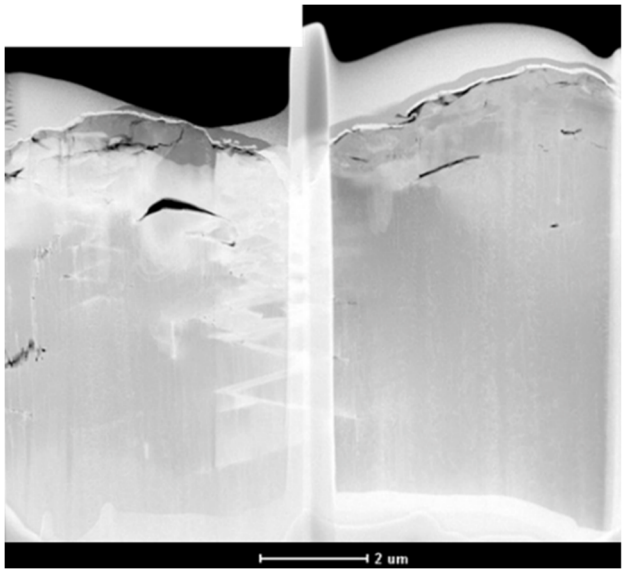

Figure 1. High-angle annular dark field cross-section image showing the surface and subsurface damage induced by wafer slicing. Cracks and voids are observed (dark contrast beneath the surface). The scale bar is 2 μm.

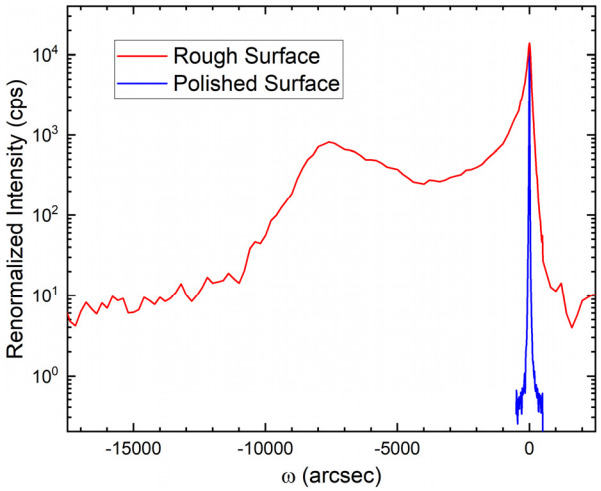

Figure 2. Triple-axis X-ray diffraction symmetric (020) β-Ga_2O_3 rocking curves for the rough surface, as-received wafer sliced substrate (FWHM = 150" and low angle grain boundary at ~7600") and the polished surface after CMP (FWHM = 13").

Substrate mounting to the diffractometer stage for XRD measurements is crucial for measuring rocking curves and diffuse scatter intensity (i.e. FWXM). The symmetric (020) rocking curves for the same polished (pristine) substrate is shown in Figure 3, where the blue curve corresponds to using a strain-free mounting process and the red curve corresponds to using a wax adhesive which covered the entire backside of the substrate similar to what is used for mounting samples for CMP processing. The "CMP Mount" configuration corresponds to the same amount of adhesive wax that was also used in mounting the substrates to the polishing jig for CMP. Under the CMP Mount conditions, the adhesive distorts the substrates by bending the crystal and introducing both strain (measured along the ω:2θ scanning axis) and lattice curvature (measured along the ω scanning axis). The peak widths for the "CMP Mount" configuration are 50" and 240" for the FWHM and FW(0.001)M, respectively. The broadening contribution from lattice curvature induced by using an excessive amount of wax dominates the rocking curve and can bury the presence of subsurface lattice damage and may convolute the analysis when optimizing polishing parameters. Therefore, samples that are not dismounted from the polishing jig will exhibit excessive peak broadening associated with the mounting and not necessarily with the material crystalline quality.

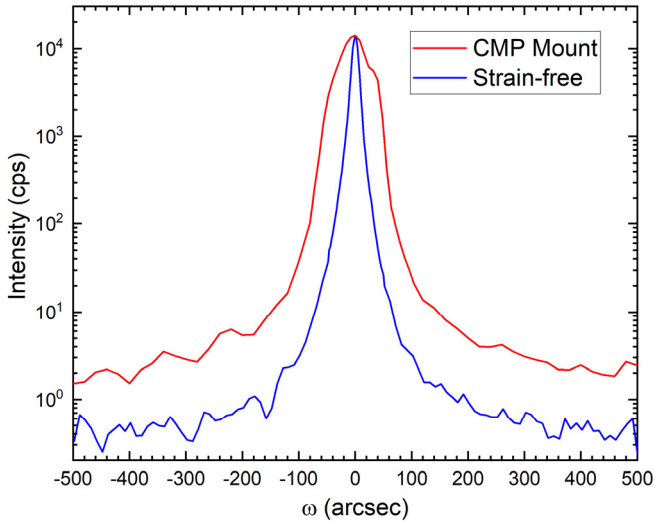

Figure 3. Triple-axis X-ray diffraction symmetric (020) β-Ga_2O_3 rocking curves for the same polished substrate: one with a strain-free mount (FWHM = 13", FW(0.001)M = 130") and the other with the CMP Mount (FWHM = 50", FW(0.001)M = 240").

The x-ray scattering equipment also plays a role in the analysis. The difference between TAXRD and double-axis XRD (DAXRD) is shown in Figure 4 for a substrate polished to a pristine state and another substrate with some subsurface lattice damage present. In the double-axis measurements shown in Figure 4(a), the FWHM and FW(0.001)M values are 25" and 410", respectively for the pristine substrate and 26" and 500" for the substrate with a small amount of subsurface damage. In contrast, for the same two substrates measured in triple-axis measurements shown in Figure 4(b), the FWHM and FW(0.001)M values are 13" and 130" for the pristine substrate and 14" and 170" for the substrate with some subsurface damage. Due to the better beam conditioning optics of triple-axis arrangement (~10"), there is no contribution from scattering along the ω:2θ scanning axis, which is why the width is narrower in triple-axis compared to double-axis. Therefore, in Figure 4(b), the peak broadening and diffuse scatter intensity is unequivocally due to lattice mosaicity from subsurface damage. Furthermore, the percent difference between the pristine and damaged substrate diffuse scatter intensity is larger in triple-axis than it is in double-axis (~30% vs ~20%, respectively).

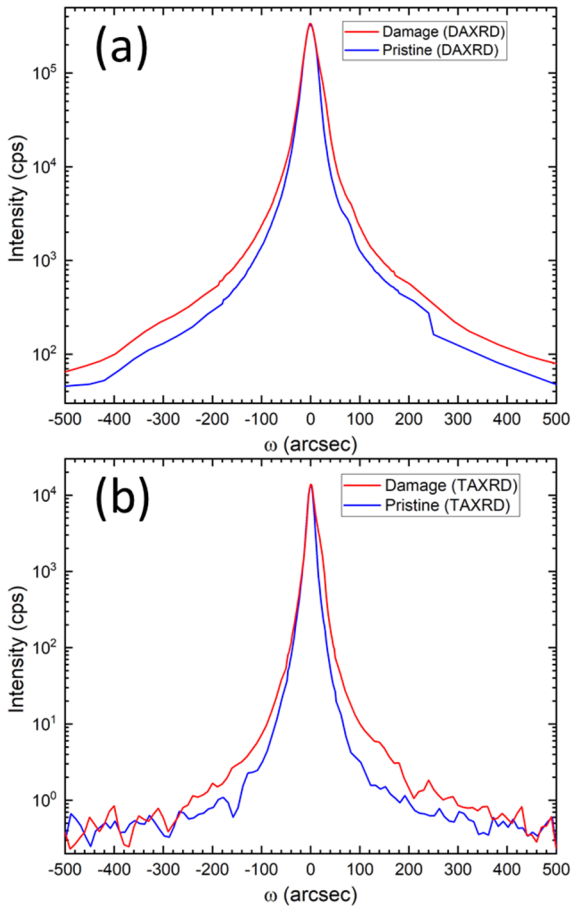

Figure 4. X-ray diffraction symmetric (020) β-Ga_2O_3 rocking curves using (a) double-axis vs (b) triple-axis geometries for one substrate polished to a damage-free state (pristine) and another substrate with some subsurface lattice damage present. The detector aperture is ~1400" and ~10" for double-axis and triple-axis, respectively.

Conclusion

Proper sample mounting technique and employing triple-axis XRD measurements are key to analyzing subsurface damage in the CMP of (010) β-Ga_2O_3 substrates. Using an excessive amount of an adhesive (e.g. the amount that can be used for mounting substrates on a polishing jig) can induce distortions that bend the substrates and artificially cause lattice curvature to dominate the XRD rocking curve peak width. Triple-axis XRD is advantageous over double-axis XRD in that lattice mosaicity measured along the ω scanning axis and peak broadening contributions from the vertical ω:2θ scanning axis are separated.

Acknowledgements

The authors would like to acknowledge the support from the Office of Naval Research through a MURI program, grant No. N00014-18-1-2429.

References

[1] M. A. Mastro, et al., ECS J. Solid State Sci. and Tech., **6**(5), P356 (2017).
[2] S. J. Pearton, et al., Appl. Phys. Rev., 5, 011301 (2018).
[3] C. Huang, et al., Precision Engineering, 56, 184 (2019).
[4] C. Huang, et al., RSC Adv., 8, 6544 (2018).
[5] S. Hayashi, et al., ECS Trans., **16**(8), 295 (2008).
[6] S. Hayashi, et al., J. Electrochem. Soc., **155**, H113 (2008).
[7] Novel Crystal Technology, Inc., https://www.novelcrystal.co.jp/
[8] M. Schuster, et al., J. Phys. D: Appl. Phys., **28**, A270 (1995).
[9] B. Poust, et al., J. Phys. D: Appl. Phys. **38**, A93 (2005).
[10] M. E. Liao, et al., ECS J. Solid State Sci. and Tech., **8**(11), P673 (2019).
[11] M. E. Liao, et al., APL Mater., **7**, 022517 (2019).

Acronyms

CMP: Chemical Mechanical Polish
TAXRD: Triple-axis X-ray Diffraction
DAXRD: Double-axis X-ray Diffraction
FWHM: Full Width at Half Maximum
FWXM: Full Width at X Maximum (X < 0.5)
cps: counts per second